Science of the Total Environment 822 (2022) 153662

Contents lists available at ScienceDirect

Science of the Total Environment

journal homepage: www.elsevier.com/locate/scitotenv

Monitoring ecosystem services in the Guangdong-Hong Kong-Macao Greater Bay Area based on multi-temporal deep learning

Yang Lu [a], Jiansi Yang [a,*], Min Peng [b], Tian Li [b], Dawei Wen [c], Xin Huang [d,e,**]

[a] School of Urban Design, Wuhan University, Wuhan 430072, China
[b] Shenyang Geotechnical Investigation & Surveying Research Institute Co., Ltd, Shenyang 110000, China
[c] School of Computer Science and Engineering, Wuhan institute of Technology, Wuhan 430074, China
[d] School of Remote Sensing and Information Engineering, Wuhan University, Wuhan 430079, China
[e] State Key Laboratory of Information Engineering in Surveying, Mapping and Remote Sensing, Wuhan University, Wuhan 430079, China

HIGHLIGHTS

- A deep learning method was proposed to achieve the multi-temporal land use/land cover mapping.
- The ecosystem has been severely impacted in GBA, especially for provisioning, regulation, and cultural services.
- Distribution of the ecosystem service budget changes in GBA shows aggregation effects and spatially positive correlation.

GRAPHICAL ABSTRACT

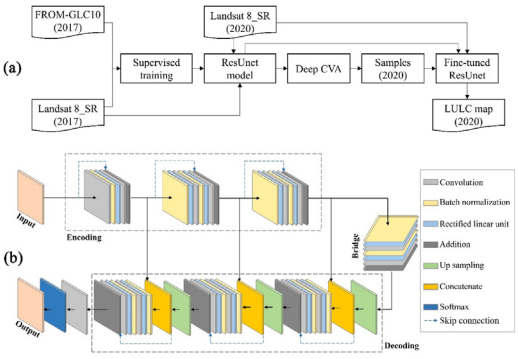

ARTICLE INFO

Article history:
Received 27 September 2021
Received in revised form 10 January 2022
Accepted 30 January 2022
Available online 3 February 2022

Editor: Martin Drews

Keywords:
Ecosystem services
Guangdong-Hong Kong-Macao Greater Bay Area (GBA)
Deep learning
Multi-temporal changes

ABSTRACT

Assessment of ecosystem service supply and demand, as well as the budgets of ecosystem service supply and demand, is the basis of scientific urban planning. In the 20 years between the proposal and formation of the Guangdong-Hong Kong-Macao Greater Bay Area (GBA), the natural ecosystem has been degraded and the ecological balance has been destroyed. In this paper, in order to assess the changes in ecosystem services in the GBA, a deep learning method composed of deep change vector analysis and the ResUnet model is proposed to achieve land use/land cover (LULC) mapping for 2000 and 2020. An index-based non-monetary evaluation method is then employed to quantify the value of the ecosystem services, and the spatial and temporal characteristics of the ecosystem service changes are analyzed. The results reveal that: (1) the proposed deep learning approach that combines deep change vector analysis (CVA) and model fine-tuning is able to achieve rapid and efficient LULC mapping in a large-scale area with multi-temporal image sequences. The overall accuracy of LULC mapping is 86.06% for 2000 and 86.67% for 2020. (2) The impervious surface area of all the cities in the GBA has increased significantly between 2000 and 2020, with an overall increase of 11.95%. (3) The mismatch between supply and demand for ecosystem services in the GBA has intensified, especially for provisioning, regulation, and cultural services. (4) The spatial distribution of the ecosystem service budget changes in the GBA shows aggregation characteristics and spatially positive correlation. These findings will provide important insights for promoting the coordinated development of the regional ecosystems and social economy in the GBA.

1. Introduction

Urbanization has become one of the most significant changes in the development of human society (Li et al., 2012). During the process of

* Corresponding author.
** Correspondence to: X. Huang, School of Remote Sensing and Information Engineering, Wuhan University, Wuhan 430079, China.
E-mail addresses: jsyang@whu.edu.cn (J. Yang), xhuang@whu.edu.cn (X. Huang).

http://dx.doi.org/10.1016/j.scitotenv.2022.153662

urbanization, natural ecosystems have been transformed into semi-natural, semi-artificial, and artificial ecosystems (Song and Deng, 2017), causing massive shrinkage of ecological land and severe environmental pollution. In this context, the structural and functional composition of ecosystems has been under great threat (Aguilera et al., 2020), leading to the loss of ecosystem service values (Fu et al., 2016). Therefore, how to coordinate the process of urbanization and ecosystem services is of great significance.

Ecosystem services reflect the knowledge and perspectives on the finiteness of natural resources and the availability of ecosystems (Feng et al., 2010). Costanza et al. (1997) considered ecosystem services as being the benefits that humans derive, either directly or indirectly, from ecosystem functions, and they estimated the economic values of 17 categories of services, including gas regulation, climate regulation, and food production. Daily (1997) defined ecosystem services as "the conditions and processes through which natural ecosystems, and the species that make them up, sustain and fulfil human life". In 2005, in order to comprehensively and systematically assess global ecosystem services from multiple scales and explore their complex impacts on human society, the United Nations launched the Millennium Ecosystem Assessment, which comprehensively discusses the concept, classification systems, impact mechanisms, evaluation techniques, and methods of ecosystem services (Chopra and Group M., 2005). In 2007, Germany and the European Commission took the lead and launched The Economics of Ecosystems and Biodiversity (TEEB) study (Bösch et al., 2018). In 2012, the United Nations approved the establishment of the Intergovernmental Science-Policy Platform on Biodiversity and Ecosystem Services (IPBES), which reflects the renewed attention to ecosystem services in the world (Borie et al., 2020). In 2014, China formally launched an assessment of the TEEB project. In 2019, the seventh session of the IPBES Plenary considered and adopted the Global Assessment Report on Biodiversity and Ecosystem Services, which is the first report to assess global biodiversity and ecosystem services (Brondízio et al., 2021). The assessment of ecosystem services can not only be used to evaluate their commodity value and promote the consideration of the ecological environment in national economic accounting systems, but it also lays the foundation for the planning of ecological environment construction and the scientific evaluation of environmental protection measures.

Scientific assessment methods are essential for evaluating ecosystem service values. At present, the commonly used methods include dynamic model assessment, physical assessment, value assessment, and index-based non-monetary evaluation. One of the most important methods of dynamic model assessment method is the Integrated Valuation of Ecosystem Services and Tradeoffs (InVEST) model. InVEST is a suite of spatially explicit ecosystem service models covering terrestrial, freshwater, marine, and coastal ecosystems, which can be used to explore the relationship, as well as the dynamics, between ecosystems and people's benefits (Tallis et al., 2015; Yang et al., 2019; Zawadzka et al., 2021). However, in this model, a number of the ecosystem service categories, such as gas regulation and climate regulation, are difficult to measure. Physical assessment is a comprehensive way of assessing the materials provided by ecosystem service functions (Feng et al., 2010; Peng et al., 2017). Nevertheless, some meteorological or ecological data are often not easy to obtain. Therefore, it is difficult to adopt physical assessment to assess the value of ecosystem services at a large scale or through multiple time series. The value assessment method translates the services provided by ecosystems into monetary values. These values reflect the overall scarcity of the service, and enable comparisons between different ecosystem services (Xie et al., 2017; Fu et al., 2016). A commonly used method of value assessment is to construct value equivalents of the various service functions in the different types of ecosystems based on land use/land cover (LULC) data, and to then evaluate the ecosystem service values based on the distribution area of the ecosystems. However, it should be emphasized that, because the natural economic values of food in the current year need to be considered, the ecosystem service values can be influenced by economic market prices. Furthermore, the value assessment method does not take into account the requirements of supply and demand. The non-monetary evaluation method represents a clear and easy-to-apply way to evaluate the budgets of ecosystem services supply and demand, which is applicable in different research areas at multiple scales. Therefore, the non-monetary evaluation method is widely used in large-scale and multi-temporal research into ecosystem services (Burkhard et al., 2012; Goldenberg et al., 2017; Tao et al., 2018).

Accurate LULC data are the basis for non-monetary evaluation, and are usually obtained by the use of a machine learning algorithm with remote sensing images (Huang et al., 2020; Yang and Huang, 2021; Yang et al., 2020a; Singh et al., 2017; Fu and Weng, 2016). Machine learning can be roughly divided into shallow learning and deep learning. Support vector machine and multilayer perceptrons are representative methods in shallow learning. In shallow learning for LULC mapping, the features need to be manually designed in advance, according to prior knowledge and experience. However, these features always suffer from poor performance and limited generalization ability. Compared to shallow learning methods, better mapping results can be obtained by applying deep learning models (Ma et al., 2019). Deep learning models can adaptively extract meaningful features in a data-driven manner (Fan et al., 2021), and can achieve an optimal model parameter configuration during the training process by simultaneously training related classifiers (Ienco et al., 2019), which greatly enhances the ability to fit complex models and avoids uncertainty. In recent years, deep learning models have been increasingly used in LULC mapping (Zhang et al., 2019; Adrian et al., 2021; Mboga et al., 2020). However, owing to the huge parameters in a deep network, a large number of samples are required (Fang et al., 2020). For multi-temporal LULC mapping over a large area, in particular, collecting sufficient training samples is time-consuming and laborious. Therefore, in this paper, we propose an approach based on information transfer from the existing thematic maps for land-cover mapping of the target year. In contrast, most studies of the dynamic monitoring of ecosystem services have used the existing land-cover datasets (e.g., the China Land Use/Cover Dataset (Song and Deng, 2017)). Land-use/land-cover data can also be generated by visual interpretation of remote sensing images (Hu et al., 2019; Jiang et al., 2019), or obtained from time-series land-use planning data (Rao et al., 2018). Deep learning, as a new mapping method, has the potential to be used for obtaining accurate time-series LULC maps, but has rarely been used to monitor ecosystem service changes. Therefore, one of the motivations of this study is to investigate the effectiveness of deep learning for ecosystem service evaluation.

The Guangdong-Hong Kong-Macao Greater Bay Area (GBA), as one of the fastest-growing regions in China, has been formed mainly over the last 20 years. The building of the Shenzhen-Hong Kong Bay Area was first proposed around the year 2000. In 2009, the planning framework for the Reform and Development of the Pearl River Delta was officially released, involving Guangzhou, Shenzhen, Zhuhai, Foshan, Jiangmen, Dongguan, Zhongshan, Huizhou and Zhaoqing, and also including Hong Kong and Macao. In the same year, a framework promoting closer cooperation between Hong Kong and Macao and a coordinated development plan for the Greater Pearl River Delta were released, with the aim being to build a world-class urban agglomeration made up of Guangdong, Hong Kong and Macao. In 2016, the 13th Five-Year Plan for Economic and Social Development of the People's Republic of China clearly stated that China would help Hong Kong and Macao to play an important role in Pan-Pearl River Delta regional cooperation, and would promote the construction of "major cooperation platforms" in the GBA (Peng, 2020). During the 20 years of the formation and development of the GBA, this region has experienced rapid social, economic, and political development, but at the same time, a series of ecological and environmental problems have emerged (Fang et al., 2019; Yang et al., 2020b; Wu et al., 2021a). In this regard, it is essential to monitor the dynamic changes of ecosystem services and promote sustainable development in the GBA.

A number of studies have been conducted with regard to the impact of urbanization on ecological and environmental quality in the GBA (Yang et al., 2020c; Zhou et al., 2018). Dynamic model assessment, physical assessment, and value assessment have all been adopted for multi-temporal dynamic monitoring of ecosystem services in the GBA (Liu et al., 2021; Wu et al., 2021b; Li and Wang, 2019). However, these methods have failed to demonstrate the supply and demand requirements of ecosystem services.

The index-based non-monetary evaluation method can directly reflect the supply and demand for different ecosystem services in different LULC categories, while providing targeted suggestions for coordinating the relationship between people's needs, economic development, and ecological environment supply. As such, the index-based non-monetary evaluation method could be used to formulate a more scientific urban planning scheme for the GBA.

In summary, the objectives of this study are: (1) to propose a deep learning method that combines deep CVA and model fine-tuning for sample transformation and LULC mapping in the GBA for the years of 2000 and 2020; (2) to quantify ecosystem service values in the GBA by linking LULC types to supply and demand matrices; and (3) to analyze the spatial and temporal characteristics of ecosystem service changes in the GBA.

2. Study area and methodology

2.1. Study area

The GBA (221°32′–24°26′N, 111°20′–115°24′E) is located in southern China, and includes nine cities (Guangzhou, Shenzhen, Foshan, Dongguan, Zhongshan, Zhuhai, Huizhou, Jiangmen and Zhaoqing) in the Pearl River Delta, as well as the Hong Kong and Macao Special Administrative Regions. According to the Outline Development Plan for the Guangdong-Hong Kong-Macao Greater Bay Area, the GBA should not only be a vibrant world-class city cluster and an important support for the construction of "the Belt and Road Initiative", but also a quality living area in which it is pleasant to live, work, and travel. However, during the development of the GBA, a large amount of natural land has been converted into construction land, and the natural ecosystem has suffered different degrees of degradation, leading to the destruction of the regional ecological balance and threats to the regional ecological security and socio-economic development. Therefore, how to ensure the sustainable provision of ecosystem services is an urgent issue for this region.

2.2. Multi-temporal LULC mapping based on deep learning

In this study, LULC maps of the GBA for 2000 and 2020 were obtained based on the FROM-GLC10 LULC product and Landsat remote sensing datasets. FROM-GLC10, which has been reported to have an overall accuracy of 72.76%, is the first global land-cover product with a 10-m resolution. The FROM-GLC10 product was produced using Sentinel-2 remote sensing datasets from 2017 (Gong et al., 2019). Compared with other LULC products, such as FROM-GLC30 (Gong et al., 2019) and the China Land Use/Cover Dataset (CLUD) (Kuang et al., 2019), FROM-GLC10 has a higher spatial resolution and provides more spatial detail information. FROM-GLC10 has been used to achieve satisfactory results in distinguishing forest from shrub and grassland classes, and it is also able to reduce the misclassification between water and shaded areas (Gong et al., 2019). In particular, FROM-GLC10 performs well in coastal areas, and is good at highlighting aquaculture activities (Gong et al., 2019). Considering these factors, FROM-GLC10 was used to collect the candidate training samples for deep learning and LULC mapping in this study. Considering the land-cover characteristics in the GBA, seven LULC types were adopted: cropland, forest, grassland, shrubland, water, impervious surface, and bareland. The Landsat remote sensing datasets were the atmospherically corrected (and almost cloud-free) Landsat 5 and Landsat 8 surface reflectance products for the GBA from the years of 2000, 2017, and 2020, which were obtained from the United States Geological Survey.

In this study, a deep learning method combining deep CVA and a fine-tuned ResUnet model was developed to achieve multi-temporal LULC mapping in the GBA. Specifically, deep CVA was used for automated sample production, and the fine-tuned ResUnet model was then employed for multi-temporal land-cover mapping.

The 2020 LULC mapping is taken as an example to illustrate the process of LULC classification in detail (Fig. 1a). The processing steps are as follows:

(1) Multi-temporal deep feature generation: The ResUnet model was trained with the 2017 Landsat images as the input features and the downsampled FROM-GLC10 maps as the training labels. The multi-temporal deep features were obtained by feeding the Landsat 8_SR image bands of 2017 and 2020 into the pre-trained ResUnet and fine-tuned ResUnet models, respectively.

The ResUnet model was chosen for the feature extraction and subsequent mapping, for the following reasons: (1) the ResUnet model is effective at representing detailed and semantic information; (2) the ResUnet model can be used to achieve pixel-wise classification; and (3) the ResUnet model contains skip connections for preserving the details of the features, while simplifying the training of the deep network and reducing the parameters (He et al., 2016; Zhang et al., 2018; Waldner and Diakogiannis, 2020; Wen et al., 2021). The ResUnet model synthesizes the advantages of U-Net and deep residual networks. It not only combines low-level detail information and high-level semantic information, but also ensures a better performance in semantic segmentation (Qi et al., 2020). Therefore, ResUnet was used as the basic network structure.

U-Net is a classical network for image semantic segmentation based on a fully convolutional neural network, which consists of a contracting path and an expansive path (Ronneberger et al., 2015). Compared with the traditional fully convolutional neural networks, U-Net combines low-level contextual information and high-level semantics to achieve full feature extraction by using the low-level detail information while retaining the high-level semantic information through stronger linkages between layers (Xu et al., 2021; Flood et al., 2019).

Increasing the depth (i.e., number of layers) of a neural network can improve the performance. Nevertheless, the deeper the network is, the more obvious the gradient disappearance can be. This phenomenon can hinder the training and lead to poor training and degradation of the network. To deal with this issue, the residual neural network architecture was proposed by He et al. (2016).

ResUnet is an architecture that combines the respective advantages of U-Net and deep residual networks. The ResUnet architecture is made up of three parts: encoder, decoder, and bridge (Fig. 1b). The first part encodes the input images into compact representations; the second part recovers the representations to pixel-wise features; and the third part acts as a bridge to connect the encoding and decoding paths.

(2) Automated production of samples: The multi-temporal deep features for 2017 and 2020 were subtracted to generate deep change vectors. The locations with a change vector magnitude less than a threshold were identified as "no-change". The labels for these no-change pixels can be conveniently obtained from FROM-GLC10. These pixels were then considered as candidate training samples for the year of 2020, since their land-cover labels were invariant between 2017 and 2020. In this way, a large number of samples were generated automatically for the 2020 LULC mapping.
(3) Generation of the LULC map for 2020: After obtaining the training samples for 2020, the fine-tuned ResUnet model was used for the 2020 LULC classification. In detail, the ResUnet model that was originally trained with the samples from 2017 was further fine-tuned to make it more suitable for LULC mapping in 2020 with the samples from 2020.
(4) Generation of the LULC map for 2000: the same procedure as described above was used for automatically generating the LULC classification result for 2000, through the deep CVA and the deep learning model fine-tuned with the samples from 2000.

Thus, a deep learning method that combines deep CVA and a fine-tuned ResUnet model was used to obtain LULC maps for 2000 and 2020 in the GBA. The proposed method can not only solve the problem of acquiring a large number of training samples in deep learning, but it can also boost the mapping accuracy by adopting an effective deep neural network.

2.3. Assessment of the capacity of the ecosystem services

Different LULC types have different ecosystem functions, depending on their structure and formation processes. The changes of land use and land

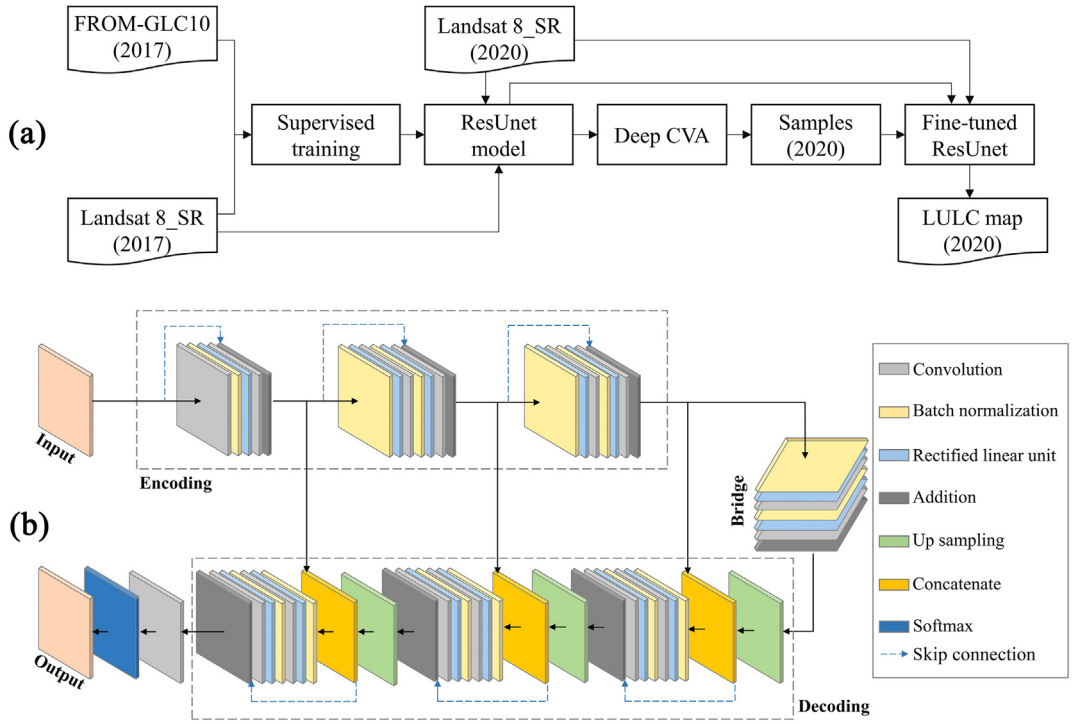

Fig. 1. (a) The proposed framework for deep learning based LULC mapping. (b) The architecture of ResUnet.

cover have a strong influence on ecosystem integrity, leading to an increase or decrease in the supply of certain ecosystem services on which human society depends. Based on the existing studies (Burkhard et al., 2012; Goldenberg et al., 2017; Tao et al., 2018; Huang et al., 2019a), seven LULC classes with three ecosystem service categories and 22 ecosystem service subcategories were used to create a supply and demand matrix for ecosystem services in the GBA.

An assessment matrix illustrating the capacity of the different LULC classes to support and supply ecosystem services is provided in Table S1. An assessment matrix illustrating the demands for ecosystem services within the different LULC categories is presented in Table S2. By subtracting the values of demand from the values of supply for each LULC category, an assessment matrix of supply and demand budgets for the ecosystem services for the different LULC categories can be obtained, as shown in Table S3. The budget values reflect the supply and demand dynamics for the ecosystem services.

It can be seen that natural LULC categories (such as forest, grassland, and cropland) have higher ecosystem service supply values, especially forest and grassland (Table S1), indicating that LULC categories with less anthropogenic disturbance have higher ecosystem service supply capacities. In contrast, in human-dominated LULC categories, such as impervious surface, there is a higher value of demand (Table S2).

3. Results and discussion

3.1. Accuracy assessment of the LULC mapping

Before accuracy assessment of the mapping results, we first evaluate the quality of the training samples that were automatically obtained based on the deep change detection method. It can be seen from Table S4 that the correctness of the training samples is 91.24% and 92.01%, respectively, for the years of 2000 and 2020, which is satisfactory, in general. Most of the automatically generated samples have a correctness of over 90%, although the quality of the shrubland and bareland classes, with a correctness of 72–78%, is not as good. Considering that the training sample collection is fully automatic, and the overall accuracy is high, it can be considered that the automatic sampling strategy is feasible for mapping the LULC and monitoring the ecosystem services.

The results of the LULC classification in the GBA for 2000 and 2020 are presented in Fig. 2b. A total of 911 and 908 test samples in the LULC maps for 2000 and 2020 were randomly selected, respectively. The overall accuracy is 86.06% for 2000 and 86.67% for 2020, indicating a satisfactory classification result (Tables S5 and S6). There are seven LULC categories in the classification maps, which, therefore, theoretically, leads to 42 (7 × 6) change types. However, in fact, only five types of changes take place. Other categories rarely occur, such as shrubland to cropland, impervious surface to forest, and water to forest. Therefore, there are a total of six types of change transitions considered in this study area (including the “no-change” category). To assess the accuracy of the change detection, 90 test samples were randomly selected for each category (540 samples in total). The overall accuracy of the change detection is 83.33%, with a kappa coefficient value of 0.80 (Table S7).

To evaluate the performance of the proposed deep learning method that combines deep CVA and a fine-tuned ResUnet model, we compared it with the ResUnet model without sample transfer. Specifically, the FROM-GLC10 data were used as training labels, and the ResUnet model was directly trained to obtain the 2000 and 2020 LULC results with the same samples from FROM-GLC10. In this situation, the deep CVA method was not used for transferring the samples of 2017 to the target years (i.e., 2000 and 2020). This experiment was designed to test the efficacy of the proposed sample transfer method and multi-temporal mapping strategy. In addition, the random forest classifier was chosen as a representative classifier for the comparison with the proposed deep learning method, due to its robustness, high efficiency, and high accuracy in processing high-dimensional data (Bauer and Kohavi, 1999; Banfield et al., 2006). The effects of the random forest classifier have been extensively tested in a large number of large-scale land-cover mapping studies (Gong et al., 2019; Yang and Huang, 2021; Wang et al., 2015).

By comparing the classification results of the proposed method, ResUnet without the sample transfer and the random forest classifier (Tables S8 and S9), it can be seen that both the classification and change detection accuracy obtained by the proposed deep learning method are better than other ones. This comparison confirms the superiority of the proposed deep learning method for accurate multi-temporal LULC mapping.

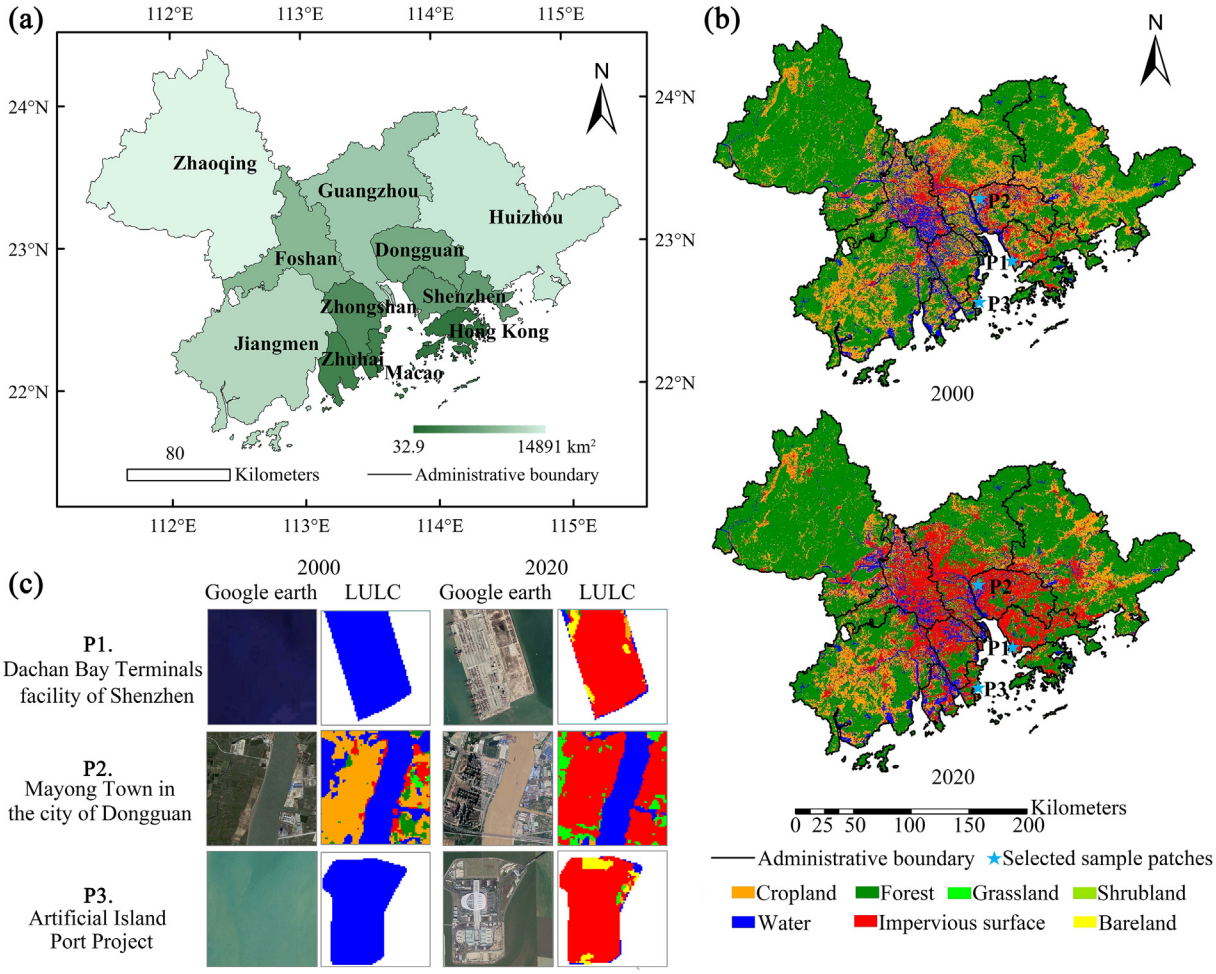

Fig. 2. (a) Overview of the study area. (b) LULC maps in the GBA for 2000 and 2020. (c) Samples of the LULC changes.

3.2. Analysis of the LULC changes

Fig. 3 shows the composition of the LULC types in 2000 and 2020 for each city in the GBA. The impervious surface areas of all the cities in the GBA increased significantly over this timeframe, with an overall increase of 11.95%. In addition, most of the newly constructed impervious surface area was transformed from cropland, forest, and water (Fig. 2b). On the one hand, it could be stated that the rapid economic development has been the main driver for the growth of the impervious surface area (Deng et al., 2018; Guo et al., 2019). According to the statistical yearbooks, from 2000 to 2020, the gross regional product (GDP) of all nine inland cities in the GBA increased by more than five times, and Hong Kong and Macao also experienced significant growth. On the other hand, in order to accommodate the urban expansion and industrial layout, the land-use planning department of each city has issued corresponding General Land Use Planning (2006–2020) documents, which put forward suggestions on land-use patterns. An orderly increase in construction land in industrial, residential, commercial, and other functional areas has resulted in the expansion of the impervious surface area.

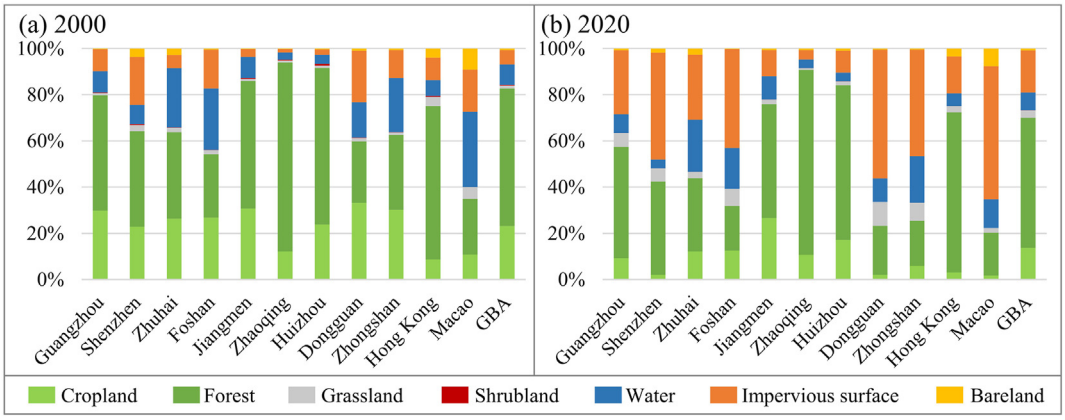

Fig. 3. Composition of the LULC types by city in the GBA for (a) 2000 and (b) 2020.

It is worth noting that the last 20 years have been a critical period for the change from the Pearl River Delta to the GBA. Relying on the geographical advantages of being adjacent to Hong Kong and Macau, as well as the corresponding supporting policies, the primary industries (i.e., agriculture and fisheries) of the inland cities have gradually transformed into secondary industries (i.e., heavy industries and manufacturing) and tertiary industries (i.e., service industries and high-tech industries), which has led to the rapid economic development. Meanwhile, according to the urban planning schemes for each city, such as the Overall Urban Planning of Shenzhen (2010 − 2020) and the Overall Urban Planning of Guangzhou (2011 − 2020), the GBA cities are taking active measures to improve the urban infrastructure by constructing public transportation facilities, airports, parking lots, and other facilities, such as the Dachan Bay Terminals facility of Shenzhen (Fig. 2c). In addition, during the process of industrial restructuring and infrastructure improvement, a large number of employment opportunities have been created by the rapid increase of the urban population and residential land, which has also led to a dramatic increase of the impervious surface areas in these inland cities, such as the new residential area in the town of Mayong in the city of Dongguan (Fig. 2c). However, due to the different levels of economic development and the different urban strategic plans, the impervious surface areas have increased to different degrees in the GBA cities. Specifically, with the smallest increment of impervious surface areas, Jiangmen, Huizhou, and Zhaoqing have increased by 8.02%, 7.21% and 2.68% respectively, while the other inland cities have all increased by more than 18%. Jiangmen and Zhaoqing are third-tier cities, and the relatively long distance from Guangzhou and Shenzhen has led to a weak radiation driving effect from the big cities. In addition, although Huizhou is a second-tier city and adjacent to Guangzhou and Shenzhen, the distance between the forest areas, such as Shimen, Nankunshan, and Jianfengshan, to a certain extent, has hindered the economic radiation effect from the first-tier cities. Therefore, the economic development of Huizhou is not as good as that of Foshan and Dongguan. Hong Kong, as a Special Administrative Region of China, has a high level of economic development and a scarcity of available land, due to the high population density, resulting in only a small change in impervious surface area (6.14%). Macau, which is also a Special Administrative Region of China, has seen a significant increase in impervious surface area (39.42%), which can mainly be attributed to the construction and reclamation of the Hong Kong-Zhuhai-Macao Bridge Artificial Island Port Project (Fig. 2c).

The cropland area in the GBA has decreased by 9.51%. Notably, the cropland areas of Guangzhou, Shenzhen, Dongguan, and Zhongshan have all reduced by more than 20%. The gradual reduction of cropland area reflects the transformation of suburban and rural areas to metropolitan areas (Huang et al., 2019a). Similarly, the degree of cropland area reduction is also related to urban development. Guangzhou, Shenzhen, and Dongguan are inland first-tier and new first-tier cities, and have the strongest economic activity. Although Zhongshan is a second-tier city, according to the Overall Urban Planning of Zhongshan City (2004–2020), it has been committed to developing high-tech industries and modern manufacturing industries, and hence it requires the construction of new impervious surfaces for the economic and industrial development. Consequently, these four cities have seen the largest reduction in cropland area.

Interestingly, forest in the GBA has decreased by only 3.17%, and nearly all the cities (except for Zhongshan) have experienced a decrease of forest of less than 10%. In the last 20 years, the GBA cities have adopted a series of policies and regulations related to forest protection, and there has been an explicit proposal to build a national forest city cluster, while the nine inland cities have been recognized as National Forest Cities and National Garden Cities. This indicates that, in the process of urban development, the conservation of forest has been strongly emphasized in the GBA cities.

3.3. Analysis of the ecosystem service changes

3.3.1. Overall change of the ecosystem services in the GBA

Table 1 lists the changes of the ecosystem services in the GBA cities from 2000 to 2020. As can be seen from the table, the ecosystem services of the GBA have undergone significant changes from 2000 to 2020. The total demand has increased by 67.17%, while the total supply and budgets have fallen by 8.22% and 30.57%, respectively. This phenomenon reveals that, during the formation and development of the GBA, the ecosystem has been severely affected, and the imbalance between supply and demand has been exacerbated.

Jiangmen, Zhaoqing, and Huizhou, as densely forested cities, account for more than 75% of the total forest area in the GBA. In addition, the ecosystem service supply value of forest reaches 71, in terms of Table S1, which is much higher than that of the other LULC types, so that the ecosystem service supply values for Jiangmen, Zhaoqing, and Huizhou account for over 15% of the GBA, and their total contribution is greater than 70%. However, the economic development of these three cities is relatively slow, and less forest has been converted to other LULC types, according to the laws and regulations for forest protection. Therefore, in these regions, the changes of ecosystem service supply, demand, and budget are the least, and the ecosystem is the most stable.

In contrast, due to the reduction of cropland, forest, and water caused by urban expansion and infrastructure construction, Shenzhen, Foshan, Dongguan, Zhongshan, and Macau have seen a significant decrease in the supply of ecosystem services and a significant increase of demand. In particular, the demand for Zhuhai, Zhongshan, and Macao has increased by more than 100%. Consequently, in 2020, the ecological supply for these five cities failed to meet their demand, and hence their ecosystem service budgets became negative.

Budgets reflect the supply and demand balance of ecosystem service values. A change in budget of less than 0 indicates that the ecosystem service is changing to a stage where demand is greater than supply. The dynamic change of the budget of each ecosystem service in the GBA from 2000 to 2020 is described in Fig. 4, including three ecosystem service categories and 22 subcategories. The three ecosystem service categories (i.e., regulating, provisioning, and cultural services) are highlighted in orange in the figure. It can be seen from Fig. 4 that all the cities show a consistent trend of change, i.e., the change values of all the service types are less than 0. Among the different types, the provisioning services show the largest degradation.

3.3.2. Change analysis of the provisioning services

Provisioning services mainly refer to services that provide food, livestock, aquatic products, and other materials, to meet the basic living requirements of residents. However, in the process of urban expansion, most of the impervious surface area has been converted from cropland, grassland, water, and other LULC types, resulting in a loss of the corresponding carriers for provisioning services. Consequently, urbanization has the most direct and significant impact on provisioning services. The reduction in the supply of provisioning services reflects the transformation of a city's industrial structure from primary to secondary and tertiary industries. The primary target of the GBA is to build a world-class city cluster, and economic development is the main goal, so the reduction of local provisioning services due to industrial restructuring seems inevitable.

Furthermore, the crops, livestock, and aquaculture services in the provisioning services category were also analyzed to reflect the agricultural situation of the GBA. Specifically, the data for the permanent population, crop production, number of slaughtered fattened hogs, and aquatic products from 2000 to 2019 in the nine inland GBA cities were obtained from the Guangdong Statistical Yearbook (http://stats.gd.gov.cn/gdtjnj/).

The population of the nine GBA inland cities has grown substantially in the last 20 years, with Shenzhen and Guangzhou as first-tier cities having the largest population growth, at over 5 million each (Fig. S1a). The decrease of cropland and the increase of impervious surface area has led to the change of food service budget being less than 0 in all nine cities,

Table 1
Ecosystem service supply, demand, and budget dynamics in the GBA as a whole and in each city.

City	Supply (%)			Demand (%)			Budget (supply − demand)		
	2020	2000	Rate	2020	2000	Rate	2020 (value)	2000 (value)	Rate (%)
Guangzhou	11.42	11.71	−10.56	17.65	16.97	73.92	117,889,078	247,662,764	−52.40
Shenzhen	2.44	2.67	−15.93	7.09	6.88	72.29	−14,803,016	34,566,505	−142.82
Zhuhai	2.03	2.32	−19.57	3.85	2.79	130.98	12,513,500	53,248,436	−76.50
Foshan	3.65	4.67	−28.38	13.52	11.74	92.45	−57,578,618	62,801,928	−191.68
Jiangmen	16.33	16.48	−9.09	14.06	15.46	52.02	303,834,167	409,309,161	−25.77
Zhaoqing	34.80	32.67	−2.24	10.91	14.16	28.79	877,803,450	930,402,373	−5.65
Huizhou	23.30	22.21	−3.70	13.98	15.52	50.63	507,103,037	589,847,670	−14.03
Dongguan	2.12	2.81	−30.68	10.71	9.68	85.02	−67,836,945	18,898,534	−458.95
Zhongshan	1.64	2.34	−35.80	6.44	4.60	134.14	−30,298,495	40,785,567	−174.29
Hong Kong	2.25	2.08	−0.38	1.64	2.11	29.83	45,570,618	50,365,596	−9.52
Macao	0.02	0.04	−40.46	0.15	0.10	154.86	−1,067,220	505,674	−311.05
GBA	100.00	100.00	−8.22	100.00	100.00	67.17	1,693,129,556	2,438,394,208	−30.57

$\text{Rate} = \frac{\text{Value}(2020) - \text{Value}(2000)}{\text{Value}(2000)} \times 100\%$

indicating that crop services are all shifting to the stage of greater demand, which coincides with the decrease of per capita crop production in most cities. As can be seen in Fig. S1b, Shenzhen is the only city with higher per capita crop production in 2019 than in 2000, which is mainly related to the change in the crop-sown area. From 2000 to 2016, the overall trend of the crop-sown area in Shenzhen decreased, but the sown area in 2017 was significantly higher. Even though the sown area decreased in 2018 and 2019, the area in 2019 was still larger than that in 2000 (Fig. S2) (http://stats.gd.gov.cn/gdtjnj/). This can be attributed to the implementation of the Structural Reform of Agriculture and Accelerating the Cultivation of New Driving Forces for Agricultural and Rural Development plan, which was issued in 2017 by the government. In general, from 2000 to 2019, the yield per mu (a mu = 0.0667 ha) in the inland GBA cities was consistently around 300 kg (http://stats.gd.gov.cn/gdtjnj/), but the significant decrease in the sown area of crops and the increase of population has led to an overall decrease in crop yield and per capita crop output.

With regard to livestock (Fig. S1c) and aquaculture (Fig. S1d) services, their budget change values are less than 0, since the land categories with higher supply capacities have been changed to those with higher demand, such as water to impervious surface. Due to the industrial transformation, the livestock production in the inland cities has declined, resulting in a decrease in the per capita number of slaughtered fattened hogs in all cities. However, some cities (i.e., Zhuhai, Zhaoqing, Zhongshan, Foshan, and Jiangmen) experienced an increase in per capita aquatic production. According to the Thirteenth Five-Year Plan for the Development of Modern Fishery in Guangdong Province, the traditional fishpond aquaculture has been gradually transformed into standardized, mechanized, and information-based aquaculture, which has improved the technical level of aquaculture production and led to a significant increase in the yield and quality of aquatic products per unit area. This phenomenon shows that the total and per capita production can be increased by improving production techniques and increasing the production per unit area.

Hong Kong and Macau put priority on the development of tertiary industries rather than primary industries, and their data for crops, livestock, and aquatic production are not available in the statistical yearbooks. Therefore, we approximated the changes in the service budgets for crops, livestock, and aquaculture by the use of their trade volumes of food imports and exports (Fig. S1e). From 2000 to 2019, the population of Hong Kong and Macau increased by 842,400 and 241,697, respectively, and the import/export food deficit of the cities increased by 75,041 million HKD and 12,597 million MOP, respectively. This indicates that, with the increase of population, Hong Kong and Macau cannot satisfy their own needs with locally produced food, and more imported food is needed, which is consistent with the changes of the service budgets for crops, livestock, and aquaculture.

In summary, with the continued socio-economic development in the GBA, the natural surfaces have been converted into impervious surfaces, and the industrial structure of the cities has been changed from primary to secondary and tertiary industries, leading to greater demand for provisioning services. In the context of the increasing population, it will be necessary to improve production technology and efficiency, and also to increase imports, in order to meet the demand.

3.3.3. Change analysis of the regulating services

From Fig. 4, it can be found that, among the regulation services, the most unbalanced supply and demand in all the GBA cities is with regard to local climate regulation and air quality regulation.

Impervious surfaces typically have a low specific heat capacity and high thermal conductivity, and can therefore absorb a large amount of thermal radiation and contribute to rapid ground warming (Lan and Zhan, 2017; Yue et al., 2019). At the same time, the vegetated areas with shade and transpiration effects often decrease over time. Moreover, industrial production and transportation often generate a large amount of anthropogenic heat, leading to significant weakening of the local climate regulation effect, which in turn further increases urban temperature. It is well known that the urban heat island effect has become one of the most prominent features of the urban climate, and can cause environmental pollution (Kleerekoper et al., 2012; Grimmond et al., 2010) and increased energy consumption (Cui et al., 2017), while posing a threat to the health of urban residents and hindering urban sustainable development. In the last 20 years, the urban heat island area in the GBA has kept increasing, and has formed an inverted "U" shaped urban heat island strip on both sides of the Pearl River Estuary (Yang et al., 2018). In addition, the natural land-cover types with cooling effects have been changed to build types with warming effects (Wang et al., 2019; Lu et al., 2021), which is consistent with the observation that all the GBA cities have more demand for local climate regulation services. In a recent study, it was shown that vegetation and water had the most dominant role in mitigating the heat island effect for the GBA cities (Lu et al., 2021). Therefore, it seems reasonable that the improvement of the local climate regulation services in the GBA cities lies in the coordinated development between natural (e.g., vegetation, water areas) and built-up land-cover categories.

The supply and demand for air quality regulation is also unbalanced. Firstly, some of the expanded impervious surface areas are used as industrial sites, where smoke is generated by burning fossil fuels and biomass. Moreover, industrial, metal, and cement dust generated from industrial production can be sources of atmospheric aerosols or suspended particulate matter (Fang et al., 2019). High aerosol concentrations reduce atmospheric visibility (Deng et al., 2008; Jung et al., 2009), and suspended particulate matter not only reduces atmospheric visibility, but is also hazardous to human health (Huang et al., 2019b). Consequently, the demand for air quality regulation has increased significantly in the GBA, but the supply of air quality regulation has decreased, due to the reduction of vegetation and the increase of the impervious surface area.

Annual average concentrations of the major air pollutants, namely, sulfur dioxide (SO_2), nitrogen dioxide (NO_2), and inhalable particulate matter

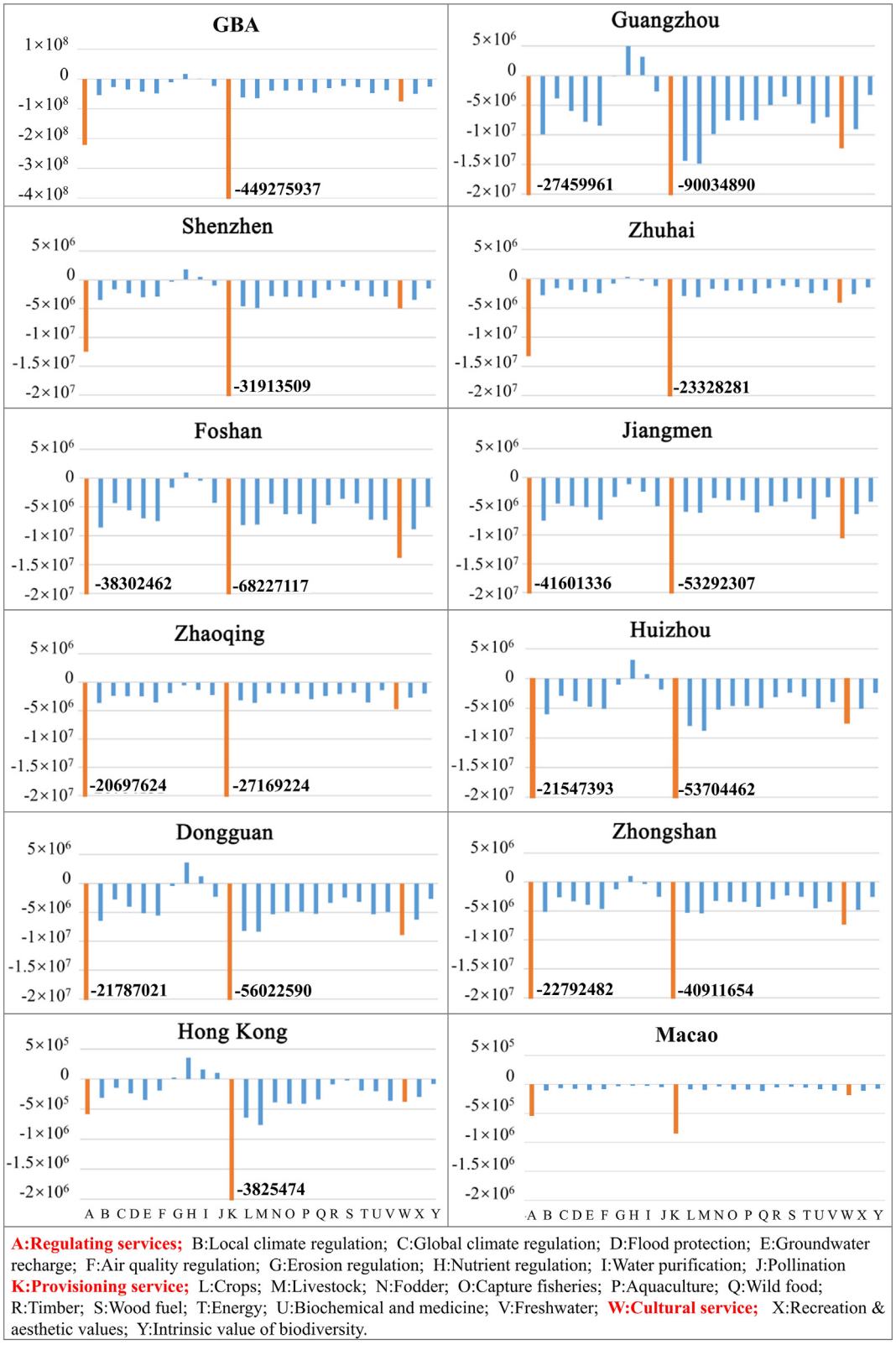

Fig. 4. Ecosystem service budget dynamics of each city in the GBA from 2000 to 2020.

(PM10), were obtained from the environmental protection departments and statistics departments, to reflect the trends of air quality changes in the GBA cities over the past 20 years (Fig. S3). According to the Ambient Air Quality Standard (GB 3095-2012) for China, the annual average concentration limits for the air pollutants of SO_2, NO_2, and PM10 in residential areas, mixed commercial traffic residential areas, cultural areas, industrial areas, and rural areas are 60 μg/m^3, 40 μg/m^3, and 70 μg/m^3, respectively.

It can be seen from Fig. S3 that all the GBA cities have shown an overall decreasing trend for air pollutant concentrations over the past 20 years. The concentration values for SO_2 and PM10 now meet the standards in 2020.

Except for Hong Kong and the North District of Macao, the concentration values of NO_2 in the other cities also reached the standard around 2020. These results demonstrate that, in the development and implementation of policies and regulations such as the Action Plan for the Prevention and Control of Air Pollution, most of the GBA cities have effectively coped with the issue of air pollution through remediation of exhaust gases, remediation of transport vehicles, renovation of high-polluting boilers, and continuous efforts to prevent dust pollution. These measures have led to an overall improvement in air quality in the GBA cities, in general. Therefore, although the impervious surface area has increased and human activities have intensified in the GBA cities, the air quality has been effectively improved through a series of control measures.

3.4. Spatial analysis of changes in the ecosystem service budgets

Due to the different economic levels and industrial structures in each region, the changes of the ecosystem service budgets in the GBA cities show different spatial distributions. The difference of the ecosystem budgets between 2000 and 2020 is used to show the spatial distribution of the ecosystem budget changes in the GBA in Fig. 5a. Subsequently, the values of the budget changes for each city were used to produce the area composition and intensity map (Fig. 5b and c). The red areas in Fig. 5a represent the areas where the budgets are less than 0 (i.e., "demand > supply"). In contrast, the green regions denote "supply > demand". For example, the total ecosystem service supply and demand values per unit area of forest are 71 and 3, respectively, and those of impervious surface are 1 and 80, respectively. Therefore, the budget values for the ecosystem services per unit area of forest and impervious surface are 68 and −79, respectively. When forest is converted to impervious surface, the change value in the ecosystem service budget per unit area is 147, indicating that the demand has reached the maximum. In contrast, when impervious surface is transferred to forest, the change value in the ecosystem service budget per unit area is −147, indicating that the supply is at its maximum. The gray, blue, and green areas in Fig. 5b and c represent the area composition ratios of areas where the budget is less than 0, unchanged, and greater than 0, respectively.

The "demand > supply" areas are mainly concentrated in the central regions of the GBA, since the central areas (e.g., Guangzhou and Shenzhen) are the engines of regional development. Driven by the economic radiation effect of Guangzhou and Shenzhen, their adjacent cities also have a high level of economic development, and their urban areas have increased rapidly, where more natural surfaces (e.g., forest and grass) with high ecosystem service supply have been converted into impervious surface. From Fig. 5b, it can be seen that the city that has the largest area of "demand > supply" is Jiangmen. In addition to the conversion of natural land surface to impervious surface, in Jiangmen, there has also been some conversion of forest to cropland and other natural surfaces with low ecosystem service supply capacity. Fig. 5 c shows the area composition (or ratios) of budget dynamics for each city in the GBA, reflecting the intensity of the budget dynamics. The ratio of "demand > supply" in Macao and Zhongshan reaches 47.51% and 44.73%, respectively, while the ratio is only 8.82% in Zhaoqing. This phenomenon reveals that the city with the greatest intensity of budget change is Macao, followed by Zhongshan, while Zhaoqing has the smallest intensity.

On the other hand, the "supply > demand" area accounts for 10% of the total area of the GBA, where surfaces with low ecosystem service value (e.g., bareland and shrubland) have been converted into those with high ecosystem service (e.g., grassland and forest). It can be seen that the city with the largest area and greatest intensity of "supply > demand" is Guangzhou (Fig. 5b and c), indicating that this city has achieved the greatest ecosystem restoration.

To further quantify the spatial distribution characteristics of the ecosystem service budget dynamics, we conducted a spatial analysis of the budget dynamics. By referring to the relevant literature (Hu et al., 2019), a series of grid sizes were chosen, i.e., 600 m, 900 m, and 1200 m. The global Moran's I index was calculated to explore the global spatial distribution characteristics of the service budgets. The *p*-values are 0 for all three grid sizes, and the

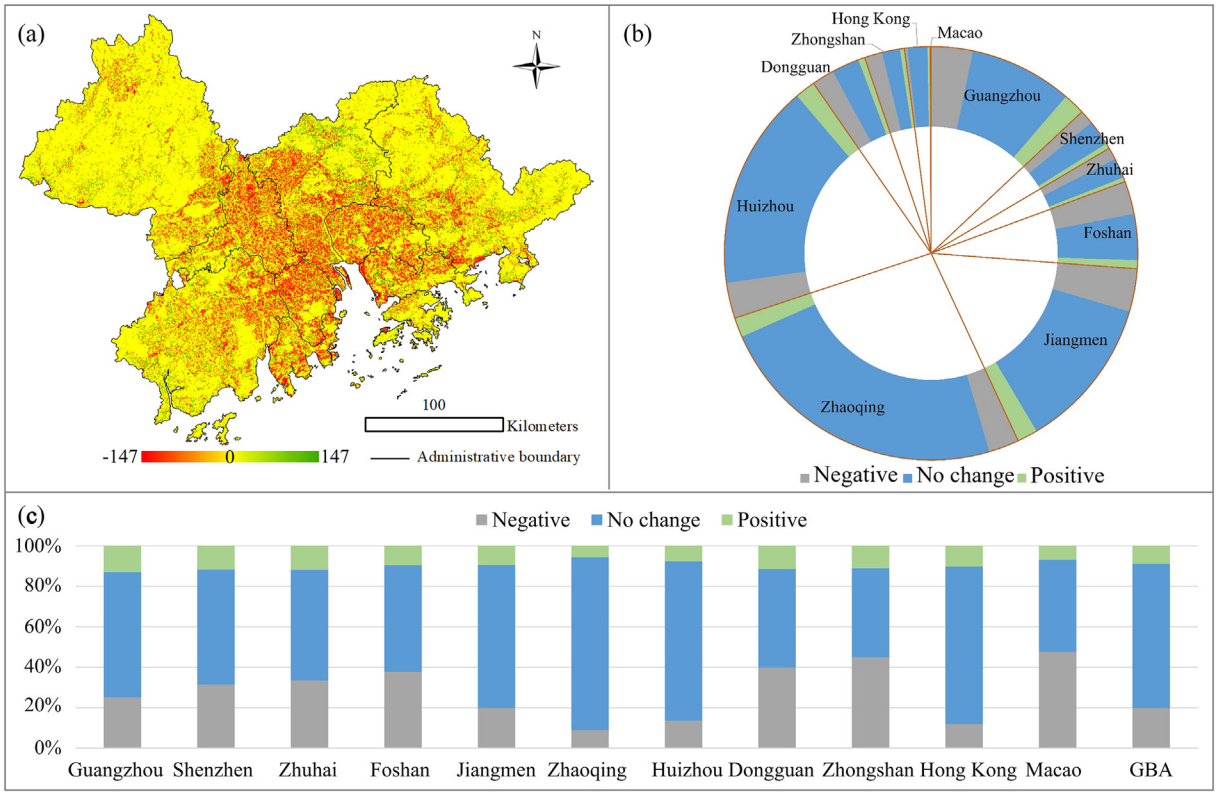

Fig. 5. (a) Spatial distribution, (b) area composition and (c) intensity of the ecosystem service budget dynamics from 2000 to 2020.

Moran's I is 0.375, 0.425, and 0.528 for the grid sizes of 600 m, 900 m, and 1200 m, respectively. Therefore, 1200 m was selected as the analysis unit in this study. The Moran's I index for the 1200 m grid size is 0.528, indicating that the dynamics of the ecosystem service budgets have strong spatially positive correlation. Furthermore, the z-score is 621.258, which means that the spatial distribution for the dynamics of ecosystem service budgets in the GBA shows aggregation characteristics.

We also conducted a hotspot analysis (Getis-Ord Gi*) (Fig. 6). The cold spots denote clustered areas of low values, as shown in blue in the figure, while hot spots stand for high-value aggregation areas, as shown in red. Most of the urban areas have been transformed from natural land-cover categories to impervious surfaces, resulting in a greater demand for ecosystem services. Therefore, the values of the budget changes in the urban areas are relatively low (Fig. 5a), which makes the urban areas become low-value agglomerations, i.e., cold spots. In contrast, most of the natural areas are hot spots, where the supply of ecosystem services is greater than the demand. Therefore, in the cold spot areas, we should not only strengthen the ecosystem service supply by increasing natural surfaces and improving provisioning services, but we should also minimize the transformation of natural surfaces into impervious surfaces. With regard to hot spot areas, in order to optimize ecological security, we should continuously protect and restore the natural resources and maintain their supply value for the ecosystem services.

4. Conclusions

In this study, a deep learning method that combines deep CVA and the ResUnet model was developed to achieve multi-temporal LULC mapping and change detection for the GBA region between 2000 and 2020. Based on the generated LULC maps, an index-based non-monetary evaluation method was employed to quantify the value of the ecosystem services, as well as their changes. Moreover, spatio-temporal analyses of the changes in ecosystem service budgets were conducted.

Our results showed that the proposed deep learning approach is effective in obtaining accurate LULC mapping and change detection, when compared with other methods (random forest and the ResUnet model without sample transfer). Moreover, the proposed method can avoid the time-consuming sample collection for deep learning by exploiting the relevance between multi-temporal images. Based on the multi-temporal mapping results, it was found that, due to economic development, urban expansion, and industrial layout, the impervious surface areas of all the GBA cities have increased significantly, and the area of cropland in all the cities has decreased, to varying degrees. In this context, the ecosystem has been severely impacted during the formation and development of the GBA, with an increased imbalance between supply and demand, especially for provisioning, regulation, and cultural services. The dynamics of the ecosystem service budgets in the GBA show a spatial aggregation pattern. Therefore, in summary, to promote the coordinated development of the ecosystem and social economy, the LULC change between natural and impervious surfaces should be effectively monitored and managed, to maintain the balance of ecosystem service supply and demand.

CRediT authorship contribution statement

Yang Lu: Software, Validation, Formal analysis, Investigation, Writing - Original Draft, Visualization.

Jiansi Yang: Conceptualization, Writing - Review & Editing, Supervision, Funding acquisition.

Min Peng, Tian Li: Investigation, Resources.

Dawei Wen: Methodology, Validation, Data Curation.

Xin Huang: Conceptualization, Methodology, Writing - Review & Editing, Project administration, Funding acquisition.

Declaration of competing interest

The authors declare that they have no known competing financial interests or personal relationships that could have appeared to influence the work reported in this paper.

Acknowledgments

This research was supported by the National Key Research and Development Program of China under Grant 2018YFB2100500, the Foundation for Innovative Research Groups of the Natural Science Foundation of Hubei Province under Grant 2020CFA003, and the Environmental Research Project in Shenzhen City (from the Ecological Environment Bureau of Shenzhen).

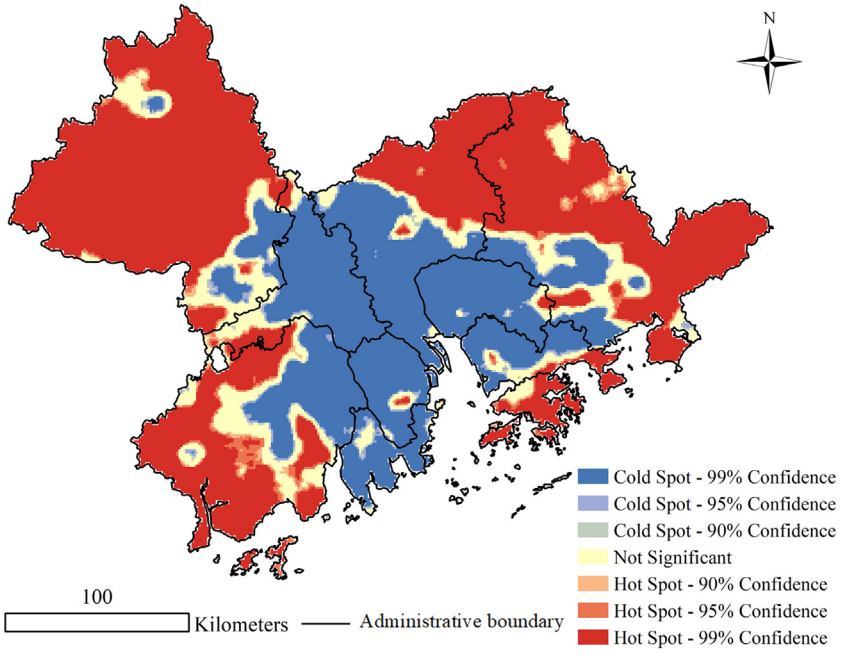

Fig. 6. Hotspot analysis of the ecosystem service budget dynamics from 2000 to 2020.

Appendix A. Supplementary data

Supplementary data to this article can be found online at https://doi.org/10.1016/j.scitotenv.2022.153662.

References

Adrian, J., Sagan, V., Maimaitijiang, M., 2021. Sentinel Sar-optical fusion for crop type mapping using deep learning and Google Earth Engine. ISPRS J. Photogramm. 175, 215–235.

Aguilera, M.A., Tapia, J., Gallardo, C., et al., 2020. Loss of coastal ecosystem spatial connectivity and services by urbanization: natural-to-urban integration for bay management. J. Environ. Manag. 276, 111297.

Banfield, R.E., Hall, L.O., Bowyer, K.W., et al., 2006. A comparison of decision tree ensemble creation techniques. IEEE Trans. Pattern Anal. Mach. Intell. 29, 173–180.

Bauer, E., Kohavi, R., 1999. An empirical comparison of voting classification algorithms: bagging, boosting, and variants. Mach. Learn. 36, 105–139.

Borie, M., Gustafsson, K.M., Obermeister, N., et al., 2020. Institutionalising reflexivity? Transformative learning and the intergovernmental science-policy platform on biodiversity and ecosystem services (IPBES). Environ. Sci. Policy 110, 71–76.

Bösch, M., Elsasser, P., Franz, K., et al., 2018. Forest ecosystem services in rural areas of Germany: insights from the national TEEB study. Ecosyst. Serv. 31, 77–83.

Brondízio, E.S., Settele, J., Diaz, S., et al., 2021. Global Assessment Report On Biodiversity and Ecosystem Services of the Intergovernmental Science-Policy Platform On Biodiversity and Ecosystem Services.

Burkhard, B., Kroll, F., Nedkov, S., et al., 2012. Mapping ecosystem service supply, demand and budgets. Ecol. Indic. 21, 17–29.

Chopra, K.R., Group M., 2005. Policy Responses: Findings of the Responses Working Group of the Millennium Ecosystem Assessment. Island Press.

Costanza, R., Arge, Groot R.D., et al., 1997a. The value of the world's ecosystem services and natural capital. Nature 387, 253–260.

Cui, Ying, Yan, 2017. Temporal and Spatial Characteristics of the Urban Heat Island in Beijing and the Impact On Building Design and Energy Performance.

Daily, G.C., 1997. Nature's Services: Societal Dependence on Natural Ecosystems. Island Press, Washington.

Deng, X., Tie, X., Wu, D., et al., 2008. Long-term trend of visibility and its characterizations in the Pearl River Delta (PRD) Region, China. Atmos. Environ. 42, 1424–1435.

Deng, Y., Fu, B., Sun, C., 2018. Effects of urban planning in guiding urban growth: evidence from Shenzhen, China. Cities 83, 118–128.

Fan, Y., Ding, X., Wu, J., et al., 2021. High spatial-resolution classification of urban surfaces using a deep learning method. Build. Environ. 200, 107949.

Fang, X., Fan, Q., Liao, Z., et al., 2019. Spatial-temporal characteristics of the air quality in the Guangdong－Hong Kong－Macau Greater Bay Area of China during 2015–2017. Atmos. Environ. 210, 14–34.

Fang, B., Li, Y., Zhang, H., et al., 2020. Collaborative learning of lightweight convolutional neural network and deep clustering for hyperspectral image semi-supervised classification with limited training samples. ISPRS J. Photogramm. 161, 164–178.

Feng, X., Fu, B., Yang, X., et al., 2010. Remote sensing of ecosystem services: an opportunity for spatially explicit assessment. Chin. Geogr. Sci. 20, 522–535.

Flood, N., Watson, F., Collett, L., 2019. Using a U-net convolutional neural network to map Woody vegetation extent from high resolution satellite imagery across Queensland. Australia. Int J Appl Earth Obs 82, 101897.

Fu, P., Weng, Q., 2016. A time series analysis of urbanization induced land use and land cover change and its impact on land surface temperature with landsat imagery. Remote Sens. Environ. 175, 205–214.

Fu, B., Li, Y., Wang, Y., et al., 2016. Evaluation of ecosystem service value of riparian zone using land use data from 1986 to 2012. Ecol. Indic. 69, 873–881.

Goldenberg, R., Kalantari, Z., Cvetkovic, V., et al., 2017. Distinction, quantification and mapping of potential and realized supply-demand of flow-dependent ecosystem services. Sci. Total Environ. 593–594, 599–609.

Gong, P., Liu, H., Zhang, M., et al., 2019. Stable classification with limited sample: transferring a 30-M resolution sample set collected in 2015 to mapping 10-M resolution global land cover in 2017. Sci. Bull. 64, 370–373.

Grimmond, C.S.B., Roth, M., Oke, T.R., et al., 2010. Climate and More Sustainable Cities: Climate Information for Improved Planning and Management of Cities (Producers/Capabilities Perspective) 1, 274.

Guo, L., Liu, R., Men, C., et al., 2019. Quantifying and simulating landscape composition and pattern impacts on land surface temperature: a decadal study of the rapidly urbanizing city of Beijing, China. Sci. Total Environ. 654, 430–440.

He, K., Zhang, X., Ren, S., et al., 2016. Deep residual learning for image recognition. IEEE Conference on Computer Vision & Pattern Recognition.

Hu, M., Li, Z., Wang, Y., et al., 2019. Spatio-temporal changes in ecosystem service value in response to land-use/cover changes in the Pearl River Delta. Resour. Conserv. Recycl. 149, 106–114.

Huang, X., Cai, Y., Li, J., 2019b. Evidence of the mitigated urban particulate matter island (UPI) effect in China during 2000–2015. Sci. Total Environ. 660, 1327–1337.

Huang, X., Han, X., Ma, S., et al., 2019a. Monitoring ecosystem service change in the City of Shenzhen by the use of high-resolution remotely sensed imagery and deep learning. Land Degrad. Dev. 30, 1490–1501.

Huang, X., Wang, Y., Li, J., et al., 2020. High-resolution urban land-cover mapping and landscape analysis of the 42 major cities in China using Zy-3 satellite images. Sci. Bull. 65, 1039–1048.

Ienco, D., Interdonato, R., Gaetano, R., et al., 2019. Combining Sentinel-1 and Sentinel-2 satellite image time series for land cover mapping via a multi-source deep learning architecture. ISPRS J. Photogramm. 158, 11–22.

Jiang, Z., Sun, X., Liu, F., et al., 2019. Spatio-temporal variation of land use and ecosystem service values and their impact factors in an urbanized agricultural basin since the reform and opening of China. Environ. Monit. Assess. 191.

Jung, J., Lee, H., Kim, Y.J., et al., 2009. Aerosol chemistry and the effect of aerosol water content on visibility impairment and radiative forcing in Guangzhou during the 2006 Pearl River Delta campaign. J. Environ. Manag. 90, 3231–3244.

Kleerekoper, L., van Esch, M., Salcedo, T.B., 2012. How to make a city climate-proof, addressing the urban heat island effect. Resour. Conserv. Recycl. 64.

Kuang, W., Zhang, S., Li, X., et al., 2019. A 30-meter resolution national urban land-cover dataset of China, 2000–2015. Earth Syst. Sci. Data Discuss. 1–33.

Lan, Y., Zhan, Q., 2017. How do urban buildings impact summer air temperature? The effects of building configurations in space and time. Build. Environ. 125, 88–98.

Li, J., Wang, J., 2019. Identification, classification and mapping of coastal ecosystem services of the Guangdong, Hong Kong and Macao Great Bay Area. Acta Ecol. Sin. 39, 6393–6403.

Li, Y., Li, Y., Zhou, Y., et al., 2012. Investigation of a coupling model of coordination between urbanization and the environment. J. Environ. Manag. 98, 127–133.

Liu, Z., Wu, R., Chen, Y., et al., 2021. Factors of ecosystem service values in a fast-developing region in China: insights from the joint impacts of human activities and natural conditions. J. Clean. Prod. 297, 126588.

Lu, Y., Yang, J., Ma, S., 2021. Dynamic changes of local climate zones in the Guangdong-Hong Kong–Macao Greater Bay Area and their spatio-temporal impacts on the surface urban heat island effect between 2005 and 2015. Sustainability-Basel 13, 6374.

Ma, L., Liu, Y., Zhang, X., et al., 2019. Deep learning in remote sensing applications: a meta-analysis and review. ISPRS J. Photogramm. 152, 166–177.

Mboga, N., Grippa, T., Georganos, S., et al., 2020. Fully convolutional networks for land cover classification from historical panchromatic aerial photographs. ISPRS J. Photogramm. 167, 385–395.

Peng, X., 2020. Research on Morphology Evolution and Spatial Model in Agglomeration of the Pearl River Estuary Bay-Area. 272. South China University of Technology Doctor.

Peng, J., Tian, L., Liu, Y., et al., 2017. Ecosystem services response to urbanization in metropolitan areas: thresholds identification. Sci. Total Environ. 607–608, 706–714.

Qi, W., Wei, M., Yang, W., et al., 2020. Automatic mapping of landslides by the ResU-Net. Remote Sens-Basel 12, 2487.

Rao, Y., Zhou, M., Ou, G., et al., 2018. Integrating ecosystem services value for sustainable land-use management in semi-arid region. J. Clean. Prod. 186, 662–672.

Ronneberger, O., Fischer, P., Brox, T., 2015. U-Net: Convolutional Networks for Biomedical Image Segmentation. Springer, Cham, pp. 234–241.

Singh, P., Kikon, N., Verma, P., 2017. Impact of land use change and urbanization on urban heat island in Lucknow City, Central India. A remote sensing based estimate. Sustain. Cities Soc. 32, 100–114.

Song, W., Deng, X., 2017. Land-use/land-cover change and ecosystem service provision in China. Sci. Total Environ. 576, 705–719.

Tallis, H., Kennedy, C.M., Ruckelshaus, M., et al., 2015. Mitigation for one & all: an integrated framework for mitigation of development impacts on biodiversity and ecosystem services. Environ. Impact Assess. 55, 21–34.

Tao, Y., Wang, H., Ou, W., et al., 2018. A land-cover-based approach to assessing ecosystem services supply and demand dynamics in the rapidly urbanizing Yangtze River Delta Region. Land Use Policy 72, 250–258.

Waldner, F., Diakogiannis, F.I., 2020. Deep learning on edge: extracting field boundaries from satellite images with a convolutional neural network. Remote Sens. Environ. 245, 111741.

Wang, J., Zhao, Y., Li, C., et al., 2015. Mapping global land cover in 2001 and 2010 with spatial-temporal consistency at 250m resolution. ISPRS J. Photogramm. 103, 38–47.

Wang, R., Cai, M., Ren, C., et al., 2019. Detecting multi-temporal land cover change and land surface temperature in Pearl River Delta by adopting local climate zone. Urban Clim. 28, 100455.

Wen, D., Ma, S., Zhang, A., et al., 2021. Spatial pattern analysis of the ecosystem services in the Guangdong-Hong Kong-Macao Greater Bay Area using Sentinel-1 and Sentinel-2 imagery based on deep learning method. Sustainability-Basel 13, 7044.

Wu, M., Wu, J., Zang, C., 2021a. A comprehensive evaluation of the eco-carrying capacity and green economy in the Guangdong-Hong Kong-Macao Greater Bay AreaChina. J. Clean. Prod. 281, 124945.

Wu, Y., Zhang, X., Li, C., et al., 2021b. Ecosystem Service Trade-Offs and Synergies under Influence of Climate and Land Cover Change in an Afforested Semiarid Basin,China. Ecol. Eng. 159, 106083.

Xie, G., Zhang, C., Zhen, L., et al., 2017. Dynamic changes in the value of China's ecosystem services. Ecosyst. Serv. 26, 146–154.

Xu, Z., Wang, S., Stanislawski, L.V., et al., 2021. An attention U-Net model for detection of fine-scale hydrologic streamlines. Environ. Model. Softw. 140, 104992.

Yang, J., Huang, X., 2021. 30 M annual land cover and its dynamics in China from 1990 to 2019. Earth Syst. Sci. Data Discuss. 2021, 1–29.

Yang, Z., Chen, Y., Wu, Z., et al., 2018. The coupling between construction land expansion and urban heat island expansion in Guangdong- Hong Kong- Macao Greater Bay. Int. J. Geogr. Inf. Sci. 20, 1592–1603.

Yang, D., Liu, W., Tang, L., et al., 2019. Estimation of water provision service for monsoon catchments of South China: applicability of the invest model. Landsc. Urban Plan. 182, 133–143.

Yang, C., Zhang, C., Li, Q., et al., 2020b. Rapid urbanization and policy variation greatly drive ecological quality evolution in Guangdong-Hong Kong-Macau Greater Bay Area of China: a remote sensing perspective. Ecol. Indic. 115, 106373.

Yang, G., Zhao, Y., Xing, H., et al., 2020c. Understanding the changes in spatial fairness of urban greenery using time-series remote sensing images: a case study of Guangdong-Hong Kong-Macao Greater Bay. Sci. Total Environ. 715, 136763.

Yang, J., Huang, X., Tang, Q., 2020a. Satellite-derived river width and its spatio-temporal patterns in China during 1990–2015. Remote Sens. Environ. 247, 111918.

Yue, W., Liu, X., Zhou, Y., et al., 2019. Impacts of urban configuration on urban heat island: an empirical study in China mega-cities. Sci. Total Environ. 671, 1036–1046.

Zawadzka, J.E., Harris, J.A., Corstanje, R., 2021. Assessment of heat mitigation capacity of urban greenspaces with the use of invest urban cooling model, verified with day-time land surface temperature data. Landsc. Urban Plan. 214, 104163.

Zhang, Z., Liu, Q., Wang, Y., 2018. Road extraction by deep residual U-Net. IEEE Geosci. Remote Sens. Lett. 15, 749–753.

Zhang, C., Sargent, I., Pan, X., et al., 2019. Joint deep learning for land cover and land use classification. Remote Sens. Environ. 221, 173–187.

Zhou, Y., Shan, Y., Liu, G., et al., 2018. Emissions and low-carbon development in Guangdong-Hong Kong-Macao Greater Bay Area cities and their surroundings. Appl. Energ. 228, 1683–1692.